

Influence of Leaf Area Index Prescriptions on Simulations of Heat, Moisture, and Carbon Fluxes

JATIN KALA, MARK DECKER, JEAN-FRANÇOIS EXBRAYAT, ANDY J. PITMAN, CLAIRE CAROUGE,
JASON P. EVANS, AND GAB ABRAMOWITZ

*Australian Research Council Centre of Excellence for Climate Systems Science, and Climate Change Research Centre,
University of New South Wales, Sydney, New South Wales, Australia*

DAVID MOCKO

SAIC at NASA Goddard Space Flight Centre, Greenbelt, Maryland

(Manuscript received 24 April 2013, in final form 29 August 2013)

ABSTRACT

Leaf area index (LAI), the total one-sided surface area of leaf per ground surface area, is a key component of land surface models. The authors investigate the influence of differing, plausible LAI prescriptions on heat, moisture, and carbon fluxes simulated by the Community Atmosphere Biosphere Land Exchange version 1.4b (CABLEv1.4b) model over the Australian continent. A 15-member ensemble monthly LAI dataset is generated using the Moderate Resolution Imaging Spectroradiometer (MODIS) LAI product and gridded observations of temperature and precipitation. Offline simulations lasting 29 years (1980–2008) are carried out at 25-km resolution with the composite monthly means from the MODIS LAI product (control simulation) and compared with simulations using each of the 15-member ensemble monthly varying LAI datasets generated. The imposed changes in LAI did not strongly influence the sensible and latent fluxes, but the carbon fluxes were more strongly affected. Croplands showed the largest sensitivity in gross primary production with differences ranging from -90% to 60% . Plant function types (PFTs) with high absolute LAI and low interannual variability, such as evergreen broadleaf trees, showed the least response to the different LAI prescriptions, while those with lower absolute LAI and higher interannual variability, such as croplands, were more sensitive. The authors show that reliance on a single LAI prescription may not accurately reflect the uncertainty in the simulation of terrestrial carbon fluxes, especially for PFTs with high interannual variability. The study highlights that accurate representation of LAI in land surface models is key to the simulation of the terrestrial carbon cycle. Hence, this will become critical in quantifying the uncertainty in future changes in primary production.

1. Introduction

Land surface models (LSMs) describe the exchange of heat, moisture, and carbon between the land surface and atmosphere. There are a wide variety of LSMs used in both regional and global climate models, and they can vary considerably in complexity (Pitman 2003). One key aspect that differentiates LSMs is whether they include phenology and, if dynamic, whether it is prescribed or simulated. In most LSMs, phenology is represented by

the leaf area index (LAI), the total one-sided surface area of leaf per ground surface area.

LAI is critical in any LSM since it affects the albedo of the terrestrial surface and hence the amount of net radiation available to drive sensible and latent heat. LAI also affects the partitioning of net radiation between sensible and latent heat fluxes (Verstraete and Dickinson 1986) because it controls the surface area of vegetation in direct contact with the atmosphere and affects the efficiency by which water can be transferred from within the vegetation to the atmosphere. Similarly, LAI affects the terrestrial carbon balance since it affects the photosynthesis and net primary productivity of a canopy. Finally, LAI influences rainfall interception and thereby affects the partitioning of rainfall between evaporation, throughfall, and runoff.

Corresponding author address: Jatin Kala, Australian Research Council Centre of Excellence for Climate Systems Science and Climate Change Research Centre, Gate 11 Botany St., Level 4, Mathews Building, University of New South Wales, Sydney, NSW 2052 Australia.
E-mail: j.kala@unsw.edu.au; jatin.kala.jk@gmail.com

The implementation of LAI in LSMs within regional and global climate models varies widely. At one end of the spectrum, some LSMs are coupled to dynamic vegetation models (e.g., Bonan et al. 2003), whereby LAI is a prognostic variable and responds to surface climate variations. However, climate biases from the regional and global atmospheric models make the realistic simulation of LAI difficult (Liu et al. 2008). As a consequence, most LSMs do not include dynamic vegetation and instead prescribe LAI.

LAI can be prescribed according to plant functional types (PFTs) from lookup tables. These values are usually based on field observations and either held constant in time or allowed to vary seasonally. This method does not allow for interannual variability or variations within PFTs; the same PFTs at different latitudes use the same LAI. Since this is not realistic, several studies have investigated the use of satellite-derived LAI and shown improvements in the simulation of surface climatology (e.g., Pielke et al. 1997; Buermann et al. 2001). The main impediment to the use of satellite-derived LAI is the limited temporal availability of these data. There is also an inherent assumption of stationarity for future climate simulations: the assumption that the present spatial and seasonal variations in LAI are representative of the future, even though they are clearly climate dependent.

Since LAI interacts with radiation, water balance, and carbon balance it is a key parameter connecting the core components of climate and ecological modeling (Parton et al. 1996). One of the key characteristics of LAI is how it varies spatially (Bonan et al. 1993) and temporally. While LAI affects the interactions between the atmosphere at a point or grid scale (Bonan et al. 1993), this scales up to continental scales (Pitman et al. 1999) in uncoupled simulations. There is additional evidence that LAI affects the atmosphere at larger scales (Chase et al. 1996). Most recently, van den Hurk et al. (2003) demonstrated that using remotely sensed LAI in a weather forecasting system affected the surface evaporation when evaporation formed a large term in the surface energy balance. They concluded that improved estimates of LAI could be an important method for improving model estimates of evaporation.

The relationship between LAI and the terrestrial carbon balance is well documented from observational studies. Barr et al. (2004) investigated the influence of LAI on net ecosystem production in a deciduous forest in Canada and found a tight coupling between the annual maximum LAI and production. Saigusa et al. (2008) used data from flux towers and found that temperate deciduous forests showed the greatest positive net ecosystem production after leaf expansion (higher

LAI) in early summer. Duursma et al. (2009) used measurements from coniferous stands in Europe and found that LAI was a significant influence on gross primary production (GPP). Finally, Keith et al. (2012) used measurements at a single flux-tower site in Australia and focused on the carbon budget during drought years. They found that reductions in LAI due to insect attacks, in addition to drought stresses, contributed to a 26% reduction in GPP and 9% reduction in ecosystem respiration as compared to years with drought stresses alone.

Some modeling studies have investigated the influence of vegetation parameters on the simulation of terrestrial carbon fluxes and season length (e.g., White and Nemani 2003; Piao et al. 2007), but few explicitly focus on the influence of LAI versus meteorological forcing. This was recently investigated by Puma et al. (2013) in an offline LSM at four North American sites. They found that variations in LAI had a dominant control on GPP, a smaller but comparable effect on transpiration, a weak influence on total evapotranspiration, and a negligible impact on runoff. Additionally, they found that the effect of LAI on GPP is greater in energy-limited regimes as compared to moisture-limited regimes, except when vegetation exhibits little interannual variations in LAI. Hence, they conclude that an accurate representation of LAI interannual variability in LSMs is critical to accurately simulate GPP.

Overall, it is clear that the way a land surface model treats LAI is central to accurately simulating the heat, moisture, and carbon fluxes at the land surface. This paper focuses on the Community Atmosphere Biosphere Land Exchange Model (CABLE; Wang et al. 2011). CABLE does not include a dynamic vegetation model by default; hence, the spatial and temporal variation of LAI are prescribed (prognostic LAI is implemented in later versions but not currently widely used). While several studies have used CABLE to answer wide-ranging research questions (e.g., Abramowitz and Gupta 2008; Cruz et al. 2010; Q. Zhang et al. 2011; Pitman et al. 2011; Wang et al. 2012; Exbrayat et al. 2013), only few studies have examined the influence of LAI on heat, moisture, and carbon fluxes in CABLE.

Zhang et al. (2013) ran global offline simulations with CABLE and conducted a sensitivity analysis by varying several vegetation and soil parameters, including LAI, by $\pm 50\%$, 30% , and 20% of the default values. Comparison of their simulations with other models (Rodell et al. 2004; Dirmeyer et al. 2006; Jung et al. 2009) showed that the influence of LAI was most noticeable in the middle and high latitudes of the Northern Hemisphere where broadleaf forests are the dominant plant functional type. However, Zhang et al. (2013) also point out

that their imposed LAI perturbation does not necessarily reflect realistic uncertainties in estimates of LAI, so they, additionally, only focused on evapotranspiration and runoff.

Lu et al. (2013) conducted an extensive parameter sensitivity analysis of CABLE over a single year at the global scale. They found that at global scale, the most important parameter affecting GPP is the maximum carboxylation rate, followed by LAI. When analyzing each PFT separately, they also found LAI to be the second-most important parameter influencing GPP, except for evergreen broadleaf forests, whereby the initial slope of the response curve of potential electron was the second-most important factor, followed by LAI. They carried out a similar analysis for latent heat and found LAI to be the third-most important factor globally, but results varied for each PFT. Namely, LAI was the most important for deciduous needleleaf trees; second-most important for evergreen needleleaf trees; third-most important for evergreen broadleaf trees, deciduous broadleaf trees, and deciduous needleleaf trees; fourth-most important for crops; and fifth-most important for shrublands.

While the work of Zhang et al. (2013) and Lu et al. (2013) provide valuable insight into the sensitivity of CABLE to LAI and its importance relative to other model parameters, the influence of realistic interannual variations in LAI on the surface energy and carbon balance remains unknown. This study provides a method of generating LAI ensembles, based on the MODIS LAI and the observed climatology, to address this knowledge gap. The next section describes the model setup and the generation of the LAI ensemble. This is followed by an analysis of the influence of different monthly varying LAI prescriptions on CABLE-simulated surface energy and carbon fluxes.

2. Methods

a. Model description

CABLE is a land surface model designed to simulate fluxes of energy, water, and carbon at the land surface and can be run as an offline model with prescribed meteorology (e.g., Wang et al. 2011) or fully coupled to an atmospheric model within a global or regional climate model (e.g., Mao et al. 2011). CABLE is a key part of the Australian Community Climate Earth System Simulator (ACCESS; see <http://www.accessimulator.org.au>), a fully coupled earth system science model, currently being used as part of the Fifth Assessment Report (AR5) of the Intergovernmental Panel on Climate Change (IPCC). The version used in this study is CABLEv1.4b.

In CABLEv1.4b, the one-layered, two-leaf canopy radiation module of Wang and Leuning (1998) is used for sunlit and shaded leaves and the canopy micrometeorology module of Raupach (1994) is used for computing surface roughness length, zero-plane displacement height, and aerodynamic resistance. The model also consists of a surface flux module to compute the sensible and latent heat flux from the canopy and soil, the ground heat flux, as well as net photosynthesis. A soil module is used for the transfer of heat and water within the soil and snow, and an ecosystem carbon module based on Dickinson et al. (1998) is used for the terrestrial carbon cycle. A detailed description of each of the modules can be found in Kowalczyk et al. (2006) and Wang et al. (2011).

LAI in CABLE is used to compute the roughness length of vegetation and the standard deviation of vertical velocities, which are used for the formulation of aerodynamic resistances and hence influence surface energy balance calculations. It is also used to compute the total flux density of radiation for sunlit and shaded leaves within the plant canopy radiation transfer model. This influences simulations of photosynthesis, stomatal conductance, leaf temperature, and energy and carbon fluxes as CABLE performs separate calculations for sunlit versus shaded leaves (Kowalczyk et al. 2006). Finally, LAI is used in the ecosystem carbon module, where it directly influences GPP and autotrophic respiration (AR). Heterotrophic respiration (HR) is not directly driven by LAI, but by soil moisture and temperature.

b. Model setup

CABLEv1.4b was used within the National Aeronautics and Space Administration Land Information System version 6.1 (LIS-6.1; Kumar et al. 2006, 2008), a flexible software platform designed as a land surface modeling and hydrological data assimilation system. A grid resolution of $0.25^\circ \times 0.25^\circ$ was utilized, covering continental Australia. The model was forced with the Modern-Era Retrospective Analysis for Research and Applications (MERRA) reanalysis (Rienecker et al. 2011) at 3-hourly intervals and integrated from 1980 to 2008 and initialized from a previous 30-yr spinup. The forcing variables included incoming longwave and shortwave radiation, air temperature, specific humidity, surface pressure, wind speed, and precipitation. The MERRA reanalysis was bias corrected for precipitation using the Australian Bureau of Meteorology Australian Water Availability Project (BAWAP) gridded precipitation dataset (Jones et al. 2009), following Decker et al. (2013). Monthly ambient carbon dioxide concentrations were prescribed using measurements from Baring Head, New Zealand (Keeling et al. 2005).

In CABLEv1.4b, the background snow-free and vegetation-free soil albedo has to be prescribed. We used the MODIS-derived, snow-free background soil albedo data from Houldcroft et al. (2009). Bare soil regions, as defined by the International Geosphere–Biosphere Programme (IGBP) land-use classification map (used in CABLE), are assigned the mean albedo over the data period (October 2002 to December 2006), while partially vegetated pixels are assigned a soil albedo derived from a linear relationship between albedo and the normalized difference vegetation index (NDVI). A linear regression model is then used to estimate the background soil albedo corresponding to zero green LAI (Houldcroft et al. 2009). The IGBP land-use classification was used, and radiative properties, including the leaf transmittance and reflectance values in the visible, near-infrared, and thermal regions, were prescribed for each vegetation type following Avila et al. (2012). These values were obtained by adjusting estimates from Dorman and Sellers (1989) until the simulated albedo from CABLE closely approximated the MODIS-observed broadband albedo.

c. Simulations

When running CABLE at a single site, LAI can be prescribed from observations at the site (e.g., Abramowitz and Gupta 2008; Wang et al. 2011; Li et al. 2012). When running CABLE over a grid domain, LAI values are by default taken from a literature-based estimate for each PFT and are fixed in time (e.g., H. Zhang et al. 2011) or vary seasonally (Avila et al. 2012). For IPCC AR5 global climate simulations, the MODIS LAI product is used in CABLE within the ACCESS global circulation model. Since the aim of this paper is to provide better information on the sensitivity of CABLE to LAI, we use the same MODIS LAI product (Yuan et al. 2011) for our control simulation (1980–2008). This is carried out by prescribing monthly mean climatological LAI at each grid cell, based on monthly averages over the period of availability of the MODIS LAI data (2000–08).

To investigate the influence of LAI, a 15-member monthly varying (1980–2008) LAI ensemble was generated using the MODIS LAI and gridded observations of maximum (T_{\max}) and minimum (T_{\min}) temperatures and precipitation from the BAWAP (Jones et al. 2009). The goal of reconstructing the LAI was to explore the model response to reasonable estimates of LAI variability; therefore, an ensemble approach based on simple linear regression between the MODIS LAI and the BAWAP data was used.

The 8-day MODIS LAI was spatially aggregated from its original $0.05^\circ \times 0.05^\circ$ grid to the BAWAP $0.25^\circ \times 0.25^\circ$ grid by weighting each 0.05° cell by the area, summing the

twenty-five 0.05° grid cells within each 0.25° cell and finally normalizing by the total area within the course grid cell. This simple method avoids introducing unnecessary complexities that arise when the LAI is interpolated using subgrid-scale PFT distributions. The 8-day, 0.25° fields were finally averaged to the monthly means by weighting each 8-day period according to the number of days from that time span that fell within a given month.

The 15 ensemble members were generated by linearly regressing the anomalous (found by removing the mean annual cycle) monthly MODIS LAI against T_{\max} , T_{\min} , and precipitation from BAWAP at each 0.25° grid cell. The regressions were performed using data from the period 2000–08, as this period is coincident with availability of the MODIS LAI. The regressions were first performed separately for each variable and subsequently using all three variables to isolate the influence of each of T_{\max} , T_{\min} , and precipitation. Owing to the lag between precipitation and vegetation greenness metrics in southeastern Australia (Decker et al. 2013), we use a centered five-point linear regression, although similar results are obtained when only three points are included. The different sets of spatially distributed regression coefficients were calculated by randomly removing 25% of the data from each of the 15 regressions.

Data were withheld as the data training period (2000–08) occurs during a long-term, large-scale drought in Australia. Limiting the temporal data in each of the regressions allows for uncertainty due to the training period selection and creates a larger spread among the final ensemble members. The 15 ensemble estimates of anomalous LAI were created by applying each of these 15 different, spatially explicit regression coefficients for the period 1980–2008. A random Gaussian noise component with the mean and standard deviation given by the mean and standard deviation of the regression errors from each fitting was added during the construction of the LAI estimates. The added noise ensures that the errors associated with the fitting propagate to the final estimates, increase the spread between each of the ensemble members, and are consistent with the assumption that errors in LAI follow a Gaussian distribution (McColl et al. 2011). Finally, these estimates of the LAI anomalies (constructed using all three data sources) were added to the mean annual cycle of the MODIS LAI to create the final LAI ensemble members. The spatially averaged ensemble spread of the anomalous LAI, relative to (i.e., divided by) the spatially averaged ensemble mean anomaly, was 19.1% for the median, 22.9% for the mean, 0.1% for the minimum, and 133.6% for the maximum. While this range of LAI is smaller compared to the range of LAI imposed by other studies, it suits the purpose of testing the influence of

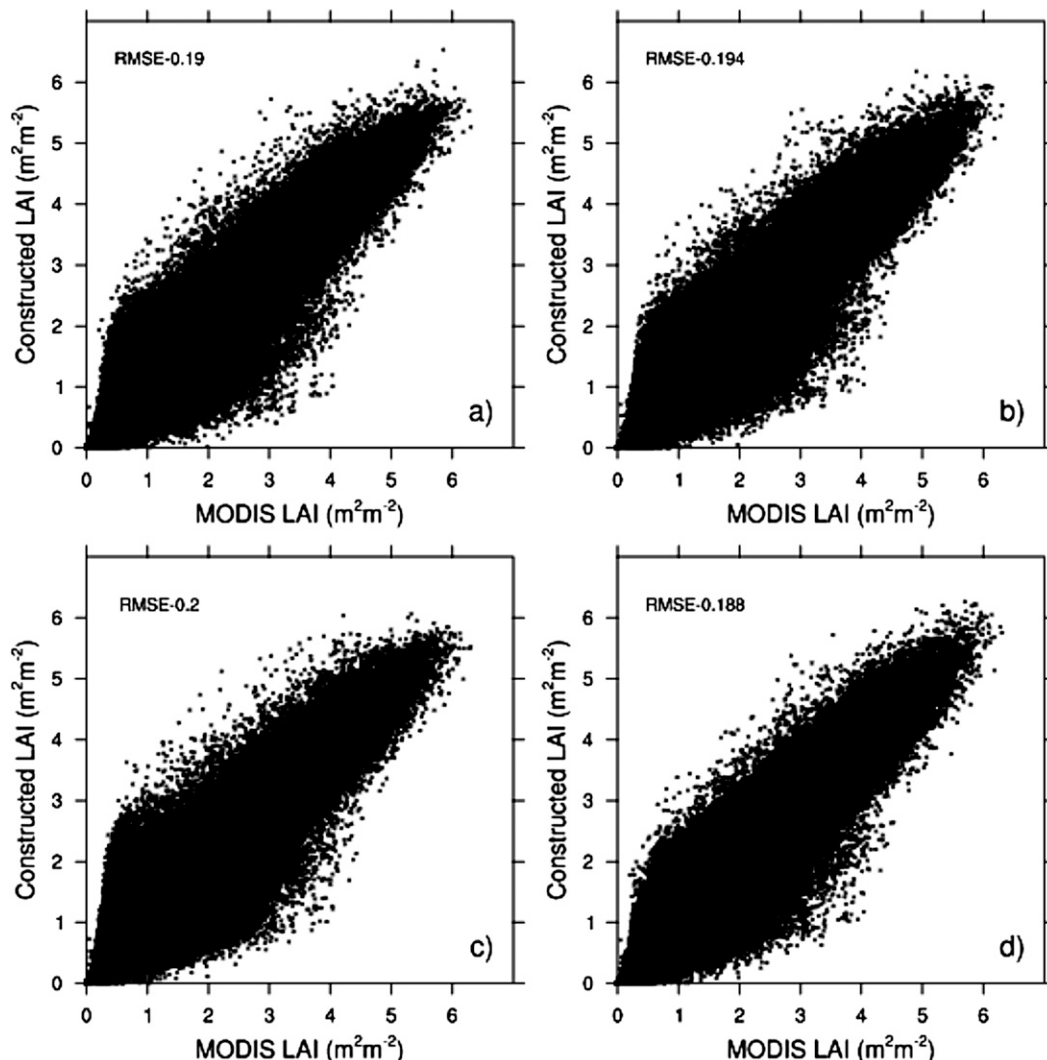


FIG. 1. Scatterplot of the ensemble mean of the constructed LAI (m^2m^{-2}) vs the MODIS LAI (m^2m^{-2}) for each grid cell for the period 2000–08 obtained using (a) precipitation; (b) T_{\min} ; (c) T_{\max} ; and (d) precipitation, T_{\max} , and T_{\min} together.

a climatologically driven LAI ensemble, which is the aim of this study.

Figure 1 shows the relationship between the MODIS LAI and the mean of the 15-member ensemble LAI reconstructions using only precipitation (Fig. 1a), T_{\max} (Fig. 1b), T_{\min} (Fig. 1c), and the combination of all three (Fig. 1d). The rms errors (RMSEs) of the single-variable regressions are 0.190, 0.194, and 0.200, respectively, while using all three variables results in a slightly better fitting (with RMSE 0.188). Figure 1 demonstrates that, while precipitation, T_{\max} , and T_{\min} can be used to reconstruct the LAI, the slope of the fittings are less than one (0.982, 0.981, and 0.980, respectively). The combination of the three (Fig. 1d) yields a slope of 0.987, which is statistically larger than the slopes of the regressions

using a single variable, but still less than one. Due to the slightly better agreement with the MODIS observations for the period 2000–08, the LAI reconstructed using all three variables was used for the model simulations. Overall, the mean of the ensemble members reconstructs the LAI variability for the period 2000–08 with R^2 values typically 0.3–0.6, with some individual ensemble members better matching the observed LAI variability over this period.

Fifteen simulations were performed over this period using these monthly varying LAI reconstructions. We note here that several studies on the influence of LAI on surface climatology use time-varying versus fixed LAI (e.g., van den Hurk et al. 2003) or apply a fixed factor [e.g., double or half LAI (Parton et al. 1996)]. Since it is

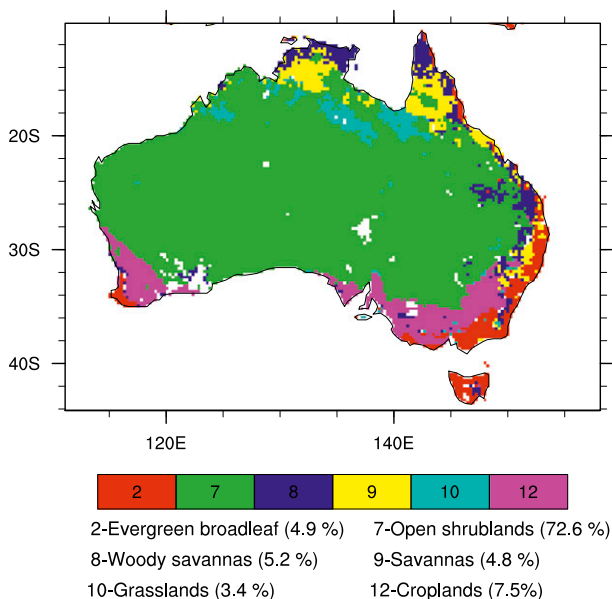


FIG. 2. Dominant plant functional types (PFTs), defined as greater than 1% of land points (masked inland regions in white are PFTs less than 1% of land points).

well established that the seasonal variation of LAI is not negligible (e.g., over croplands) and the use of remotely sensed LAI in LSMs generally improves surface climatology (Pielke et al. 1997; Buermann et al. 2001), we focus here on one of the most widely adopted remotely sensed LAI products, MODIS, and examine the sensitivity of CABLE to a MODIS-derived monthly varying ensemble LAI product, which is representative of the climatology. In summary, both the control and experiments are run over the same time period, except that the control simulation has no interannual variation in LAI while the ensemble members are designed to reflect the climatology.

d. Data analysis

The heat, moisture, and carbon fluxes were analyzed separately for each dominant PFT, defined as PFTs with coverage greater than 1% of land points, as shown in Fig. 2. This was to avoid compensating effects between PFTs, as these have distinct seasonal signals as well as absolute magnitudes. For example, croplands, being a human-managed PFT, have higher seasonal variability than native vegetation. Additionally, the dense forested areas (evergreen broadleaf trees), have the highest absolute LAI, while most of inland Australia is sparsely vegetated with open shrublands having lower absolute LAI. Since the imposed changes in LAI are on the monthly time scale, we compute monthly means and standard deviations of the fluxes and plot time series of the difference between the control and ensemble mean, with

the standard deviation used to provide a measure of spread. Since the variations in the imposed LAI vary with time (monthly) and reflect the interannual variability in climatology inherent in the BAWAP gridded precipitation and temperature dataset, we perform a time series rather than seasonal analysis (e.g., mean summer fluxes over the whole period). Additionally, we compute zero-lag cross-correlations between LAI and the fluxes to better quantify the response to changes in LAI.

3. Results

Figure 3 shows a monthly time series of the absolute (control minus ensemble mean, Fig. 3a) and the percentage difference [(absolute difference/control) \times 100, Fig. 3b] in LAI, heat, moisture, and carbon fluxes for open shrublands between 1980 and 2008. The zero-lag cross correlations with LAI are summarized in Table 1. The difference in LAI for open shrublands varies approximately between -0.2 and 0.1 , which represents a percentage change of -90% to 30% . As expected, increases in LAI lead to an increase in vegetation transpiration (EV) and a decrease in soil evaporation (ES), as shown by the strong positive cross-correlation between LAI and EV and negative correlation with ES (Table 1). Although the absolute changes in EV are smaller than ES, when expressed as a percentage change, they are larger by a factor of $\sim 2-3$. This is expected as the amount of leaf respiration is a direct function of LAI, whereas LAI only acts to partially inhibit soil evaporation.

The effects of LAI on the absolute changes in mean monthly sensible (Q_h) and latent (Q_{le}) heat fluxes are small ($<1 \text{ W m}^{-2}$), with percentage changes between -4% and 6% only, and the correlations with LAI are lower as compared to EV and ES. These small changes in Q_h and Q_{le} corresponded with equally small changes in net radiation and surface albedo (not shown). Overall surface albedo in CABLE is a function of the vegetation albedo, background snow-free soil albedo, and snow albedo. The area covered by open shrublands is not densely vegetated, so it is the background soil albedo that largely determines the overall surface albedo. The relatively small perturbation in LAI imposed did not alter the overall surface albedo to a large extent; thus, the partitioning between Q_h and Q_{le} was not generally affected.

The changes in the terrestrial carbon fluxes, on the other hand, showed a much stronger response to LAI. A decrease in LAI led to a decrease in autotrophic respiration (AR) and increase in heterotrophic respiration (HR), with strong positive cross-correlation between

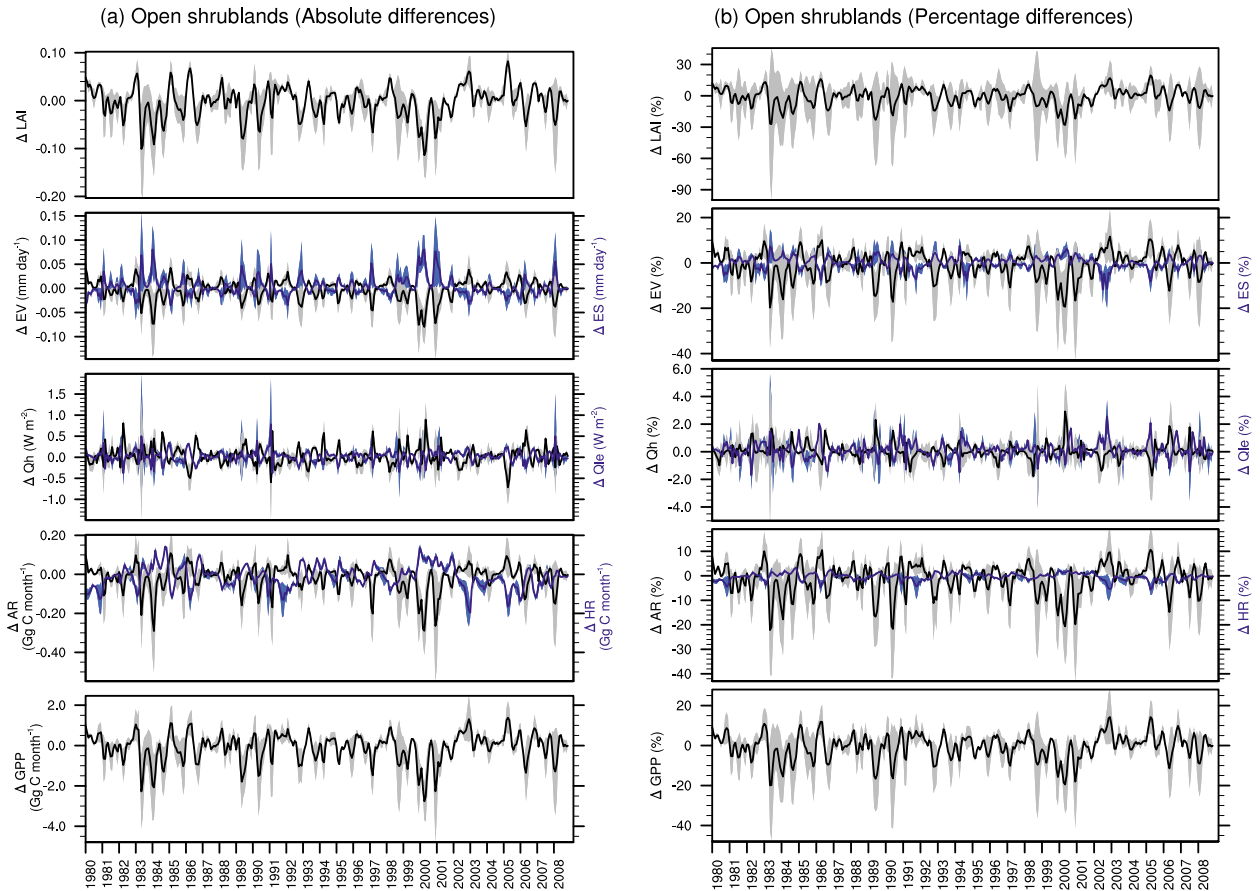


FIG. 3. Time series of (a) monthly mean absolute differences and (b) percentage differences in LAI, vegetation transpiration (EV), soil evaporation (ES), Q_h , Q_{le} , autotrophic respiration (AR), heterotrophic respiration (HR), and GPP between the control simulation and the ensemble mean for open shrublands (72.6% of land points). The shaded region represents one standard deviation.

LAI and AR and weaker negative correlation with HR (Table 1). When expressed as a percentage change, the differences in AR were up to 3–4 times larger than HR. This was expected since HR is driven by below-canopy and soil processes, while AR is a direct function of LAI. Similarly, GPP was strongly positively correlated with LAI [we note that by convention in CABLE, downward fluxes (i.e., GPP) are negative, but shown as positive here to remain consistent with the literature] as it is also a direct function of LAI, with percentage differences between -40% and 20% (the same order of magnitude as the percentage change in LAI).

For croplands (Fig. 4), the absolute change in LAI varies between -0.6 and 0.6 , corresponding to a percentage change of approximately -160% to 40% . This is larger when compared to open shrublands and all the other PFTs. Croplands, being a human-managed PFT, have the highest seasonal and interannual variation in LAI (~ 0.3 – 1.8) as compared to open shrublands (~ 0.3 – 0.5) and the other PFTs and, thus, have the strongest

response to monthly changes in precipitation, T_{max} , and T_{min} , which were used to generate the ensemble. The absolute changes in the heat and evaporative fluxes are an order of magnitude higher as compared to open shrublands (Fig. 3), and the corresponding percentage

TABLE 1. Zero-lag cross-correlations between differences in LAI and differences in vegetation transpiration (EV), soil evaporation (ES), sensible heat (Q_h), latent heat (Q_{le}), autotrophic respiration (AR), heterotrophic respiration (HR), and gross primary production (GPP) for the major plant functional types shown in Fig. 2.

PFT	EV	ES	Q_h	Q_{le}	AR	HR	GPP
Open shrublands	0.94	-0.90	-0.63	0.39	0.91	-0.76	0.99
Croplands	0.88	-0.90	0.20	-0.29	0.87	-0.56	0.95
Woody savannas	0.97	-0.88	0.31	-0.64	0.95	-0.40	0.99
Evergreen broadleaf trees	0.80	-0.88	0.63	-0.76	0.79	0.46	0.87
Savannas	0.93	-0.88	0.46	-0.65	0.91	-0.48	0.97
Grasslands	0.90	-0.80	-0.29	0.01	0.85	-0.66	0.98

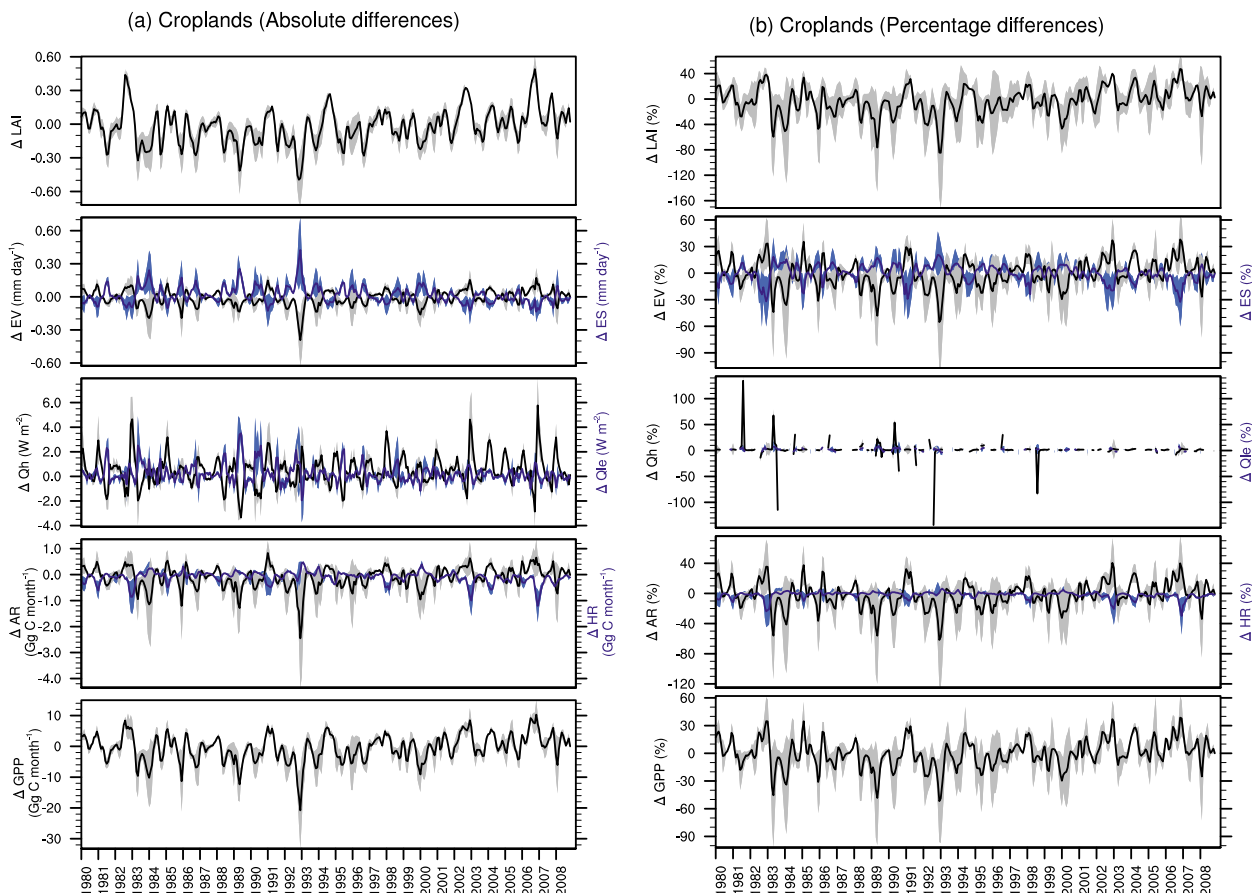


FIG. 4. As in Fig. 3, but for croplands (7.5% of land points).

changes are about double. Although the absolute changes in Q_h and Q_{le} are larger as compared to open shrublands, this change on a monthly time scale is relatively small (the large percentage changes in Q_h of up to 600% still represent a small absolute change). The small absolute LAI of croplands is such that even large percentage changes did not change the surface albedo to a large enough extent to significantly alter net radiation. The absolute changes in AR, HR, and GPP are also an order of magnitude larger compared to open shrublands, and the percentage changes are comparable to the imposed change in LAI.

The changes for the other PFTs (woody savannas, savannas, and grasslands) showed similar trends (not shown), most noticeable in the carbon, rather than the turbulent heat fluxes. Evergreen broadleaf trees (Fig. 5) had the smallest percentage change in LAI since they have the largest absolute LAI values and low interannual variability (~ 2.8 – 3.4). Therefore, this PFT had the smallest response in the carbon fluxes (-4% to 6%), with lower cross-correlations to LAI as compared to the other PFTs (Table 1). Evergreen broadleaf trees also

showed a small positive correlation to HR of 0.046 (Table 1), while all other PFTs had a negative correlation, showing that a dense canopy can enhance HR. Another noticeable result for evergreen broadleaf trees was that soil evaporation had a larger response to LAI as compared to vegetation transpiration in both absolute and percentage terms. This was a counterintuitive result, as dense forested canopies would be expected to have a larger response of vegetation evaporation to LAI compared to soil evaporation. To further investigate this, we conducted two extra simulations with large perturbations to the control LAI of $\pm 50\%$.

Figure 6 shows the seasonal difference in LAI imposed between the two experiments ($+50\%$ minus -50%) and the subsequent changes to vegetation and soil evaporation (we show contours rather than time series as the imposed LAI for these simulations has no interannual variability). As expected, a doubling of LAI results in an overall increase in vegetation transpiration and decrease in soil evaporation. However, the decrease in soil evaporation is almost twice as large as in the increase in vegetation transpiration, especially along the east coast

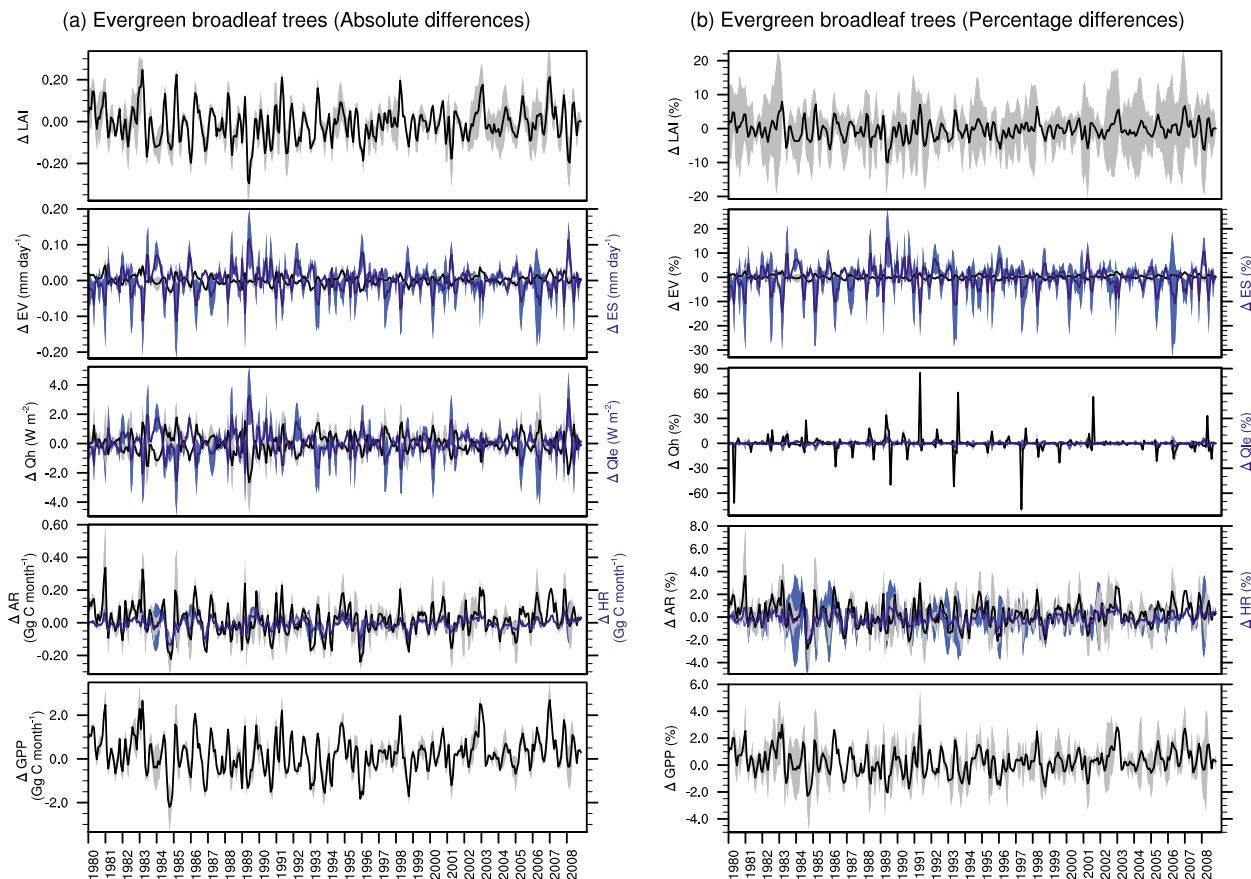


FIG. 5. As in Fig. 3, but for evergreen broadleaf trees (4.9% of land points).

where most evergreen broadleaf trees are found. This is further demonstrated in Fig. 7, showing the fraction of vegetation transpiration as a function of evapotranspiration (vegetation plus soil) for both experiments. Over a semiarid continent, changes in LAI result in a stronger response of soil evaporation as compared to vegetation transpiration.

While there are clear differences in the month-to-month variation of the heat, moisture, and carbon fluxes, increases in one period may be cancelled by a decrease later on. Additionally, we have not considered any spatial patterns in the changes in LAI and carbon fluxes. This is illustrated in Fig. 8, showing the gridded cumulative monthly mean difference in LAI on carbon fluxes (cumulative changes in LAI < 5 have been masked out to highlight the largest changes). Clearly, the largest changes in LAI and carbon fluxes are restricted to the southeastern, rather than southwestern, croplands (see Fig. 2). This is because of the imposed change in LAI being almost twice as high for the southeastern, as compared to the southwestern, croplands, as illustrated in Figs. 9a and 9b, respectively. The larger response to

LAI in the southeast is due to the larger interannual variation in precipitation in this region, which was used to generate the LAI ensemble.

4. Discussion

The literature clearly suggests that the prescription of LAI in LSMs has a strong influence on the surface heat, moisture, and carbon fluxes. Hence we conducted a series of experiments to examine the influence of LAI variability in CABLE, as it is a widely used LSM in the Australian climate community, and this sensitivity has not been previously tested.

Our results show relatively small impacts on the partitioning of available energy into the sensible and latent heat fluxes. Other studies have found much larger impacts; however, these were confined to regions of much larger changes in LAI compared to the changes imposed in this study. For example, Pitman et al. (1999) found large changes in total evaporative fluxes, but these were confined to regions where the absolute change in LAI was up to 3. Similarly, Bonan et al. (1993) found that

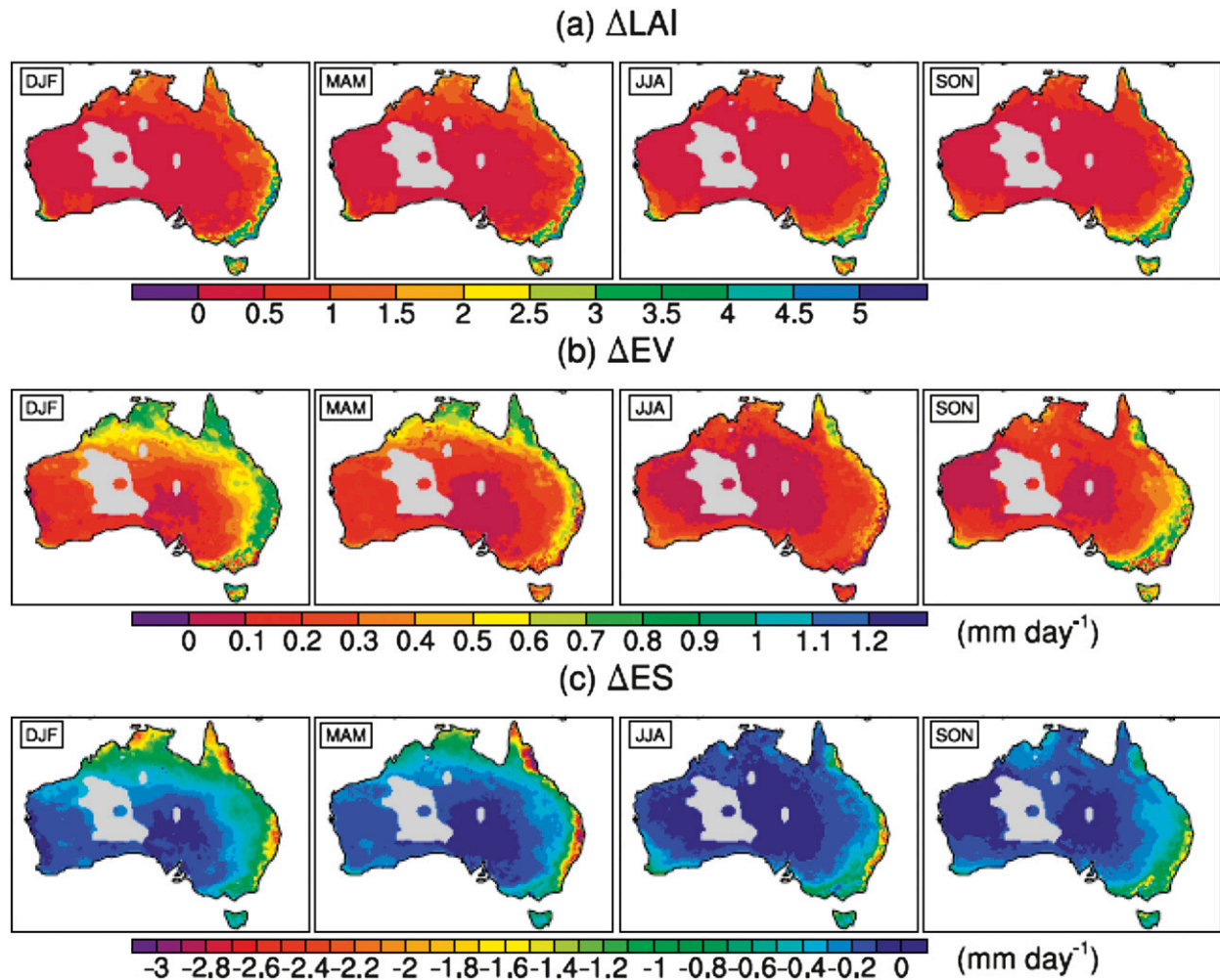


FIG. 6. Differences in (a) LAI, (b) vegetation transpiration (EV; mm day^{-1}), and (c) soil evaporation (ES; mm day^{-1}) between the experiments with +50% and -50% of the control LAI (the masked inland areas are regions where the gridded precipitation data used to generate the LAI ensemble were missing, and hence, these points were excluded from all analysis for consistency).

LAI had a strong influence on the surface energy balance, but they focused on western U.S. conifer forests, the LAI of which varies from approximately 5 to 13. The imposed changes in LAI were much smaller in magnitude but realistic and plausible, that is, related to the climatology. Even when the LAI was doubled, the magnitude of the change was less than 1 for most of the continent (Fig. 6a). Hence, the relatively small response of the evaporative fluxes is due to a small (but realistic) perturbation in LAI.

The experiments with $\pm 50\%$ of the control LAI showed that doubling LAI resulted in a decrease in soil evaporation, which is twice as large as the increase in vegetation transpiration. This result is consistent with other studies, which have shown that over half of the water lost through evapotranspiration over the Australian continent is through soil evaporation and bypasses

plants almost entirely (Haverd et al. 2013). Similar results have been found elsewhere. Namely, van den Hurk et al. (2003) showed that in relatively dry (moisture limited) areas, where LAI values are relatively low, changes in LAI cannot result in large changes in surface heat and moisture fluxes as the land surface is already constrained by available soil water. In other words, variations in LAI cause the stronger response where surface evaporation uses a large proportion of the available energy.

Van den Hurk et al. (2003) did not allow for changes in LAI to alter the surface albedo and thus omitted a feedback important to our results. In our simulations, the variations in the LAI imposed resulted in small changes in surface albedo and, subsequently, small changes in net radiation. The small change in albedo is due to the relatively small perturbation in LAI imposed

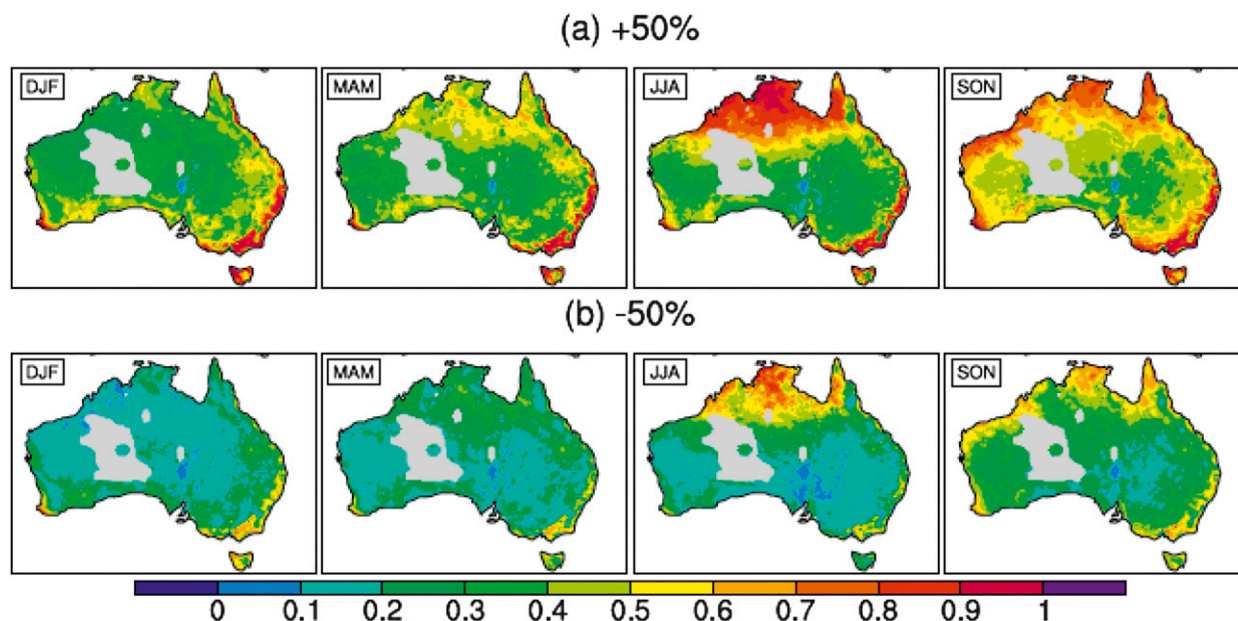


FIG. 7. Ratio of vegetation evaporation to total evapotranspiration [i.e., $EV/(ES + EV)$] for the experiments with (a) +50% and (b) -50% of the control LAI.

and because Australia is sparsely vegetated over large regions. It is therefore the background soil albedo, rather than the vegetation albedo, that has a large influence on overall surface albedo in these regions.

We found larger impacts on the terrestrial carbon balance, with LAI strongly positively correlated to gross primary production and autotrophic respiration and negatively correlated with heterotrophic respiration, consistent with both observational (Barr et al. 2004; Saigusa et al. 2008; Duursma et al. 2009; Keith et al. 2012) and modeling (Puma et al. 2013) studies that report a tight coupling between LAI and primary production. This tight coupling is not unexpected as LAI is a key variable in the parameterization of the carbon cycle. It determines not only the area of leaf that is potentially available to absorb light (and fix carbon via primary production, i.e., GPP), but also the amount of light attenuated and precipitation intercepted by the canopy. This in turn influences soil temperature, moisture, and evaporation, which drive heterotrophic respiration. However, of greater interest is the net ecosystem exchange (NEE) of carbon, that is, the difference between GPP and the sum of HR and AR. If NEE is negative, then the land surface is a net source of carbon and a sink when positive. In all our simulations, NEE was always positive for both the control and the ensemble mean; hence, the changes in LAI did not change the land surface to a source of carbon.

The largest impacts were found for croplands, which have the highest interannual variability in LAI. The changes were mostly restricted to the southeast, rather

than southwest, croplands as the imposed change in LAI was almost double in the former compared to the latter region. The southeast of Australia experiences higher interannual rainfall variability, as compared to the southwest, owing to large-scale teleconnections (Risbey et al. 2009), and this signal was reflected in the LAI ensemble produced, as it is derived using gridded, station-based precipitation and temperature data. The least impact was found for evergreen broadleaf trees, which had highest absolute LAI and lowest interannual variability. These results are consistent with Guillevic et al. (2002) and Puma et al. (2013), namely, that the impact of LAI variability is less for denser vegetation and moisture-limited regions (low evaporative fraction).

While our results are broadly consistent with existing literature, they are constrained by several caveats inherent of the study design. The model grid domain was restricted to Australia because of the spatial extent of the BAWAP precipitation and temperature data used for generating the LAI ensemble, as well as bias correcting the forcing data. Therefore, our results are largely applicable to arid and/or semiarid regions. Nonetheless, the results presented here should help inform the design of a broad range of future climate simulations whereby LAI is prescribed, especially when the focus is on the terrestrial carbon cycle. Our results are also limited to one particular LSM driven offline with a particular atmospheric forcing. Thus, our results would be worth extending via a multimodel evaluation of the sensitivity of LAI in LSMs that simulate the terrestrial carbon

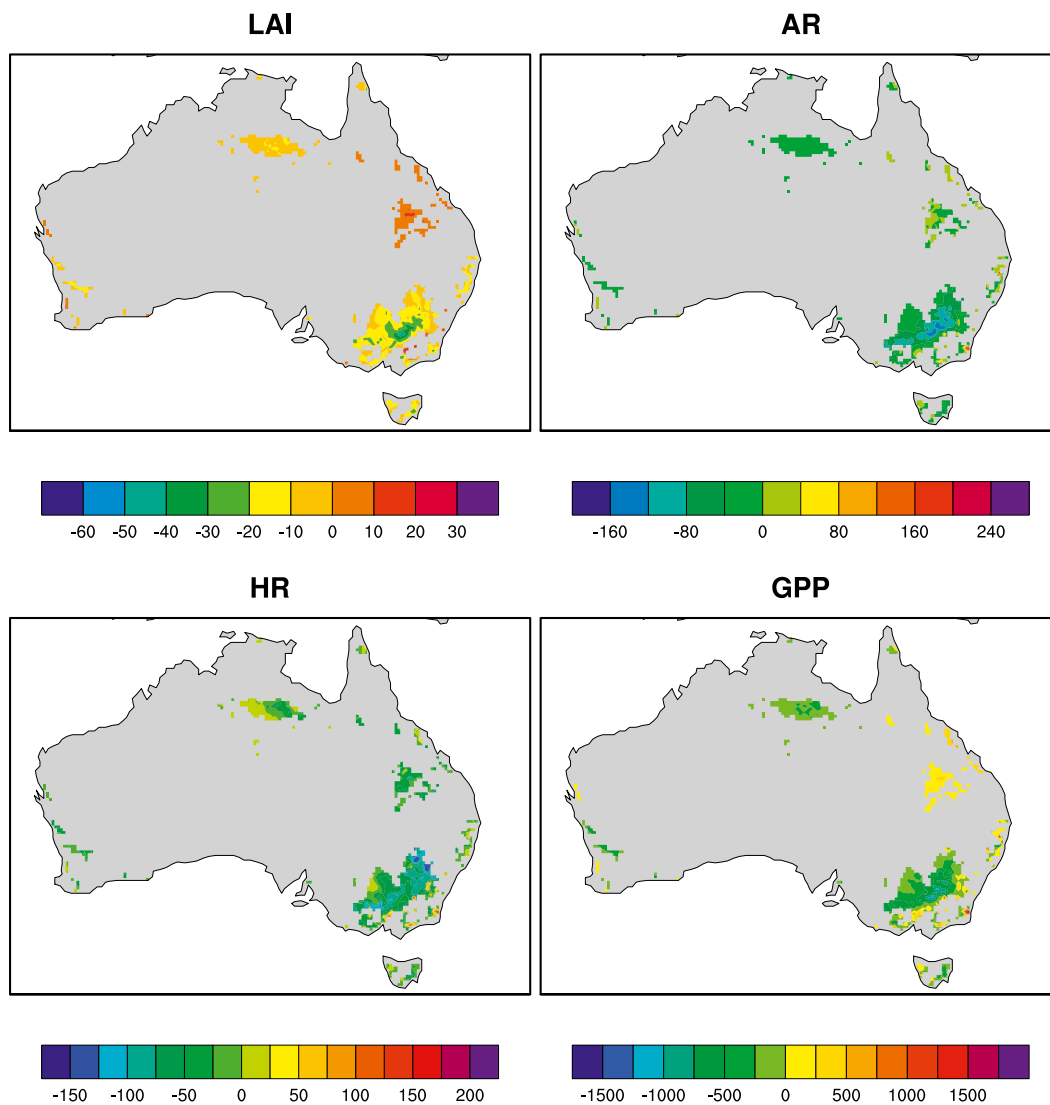


FIG. 8. Gridded cumulative difference in monthly mean LAI and carbon fluxes (Gg month^{-1}) between the control simulation and the ensemble mean (cumulative changes in LAI < 5 have been masked out to highlight the largest changes).

cycle. Despite inevitable caveats, our results highlight that the sensitivity testing of LSMs to LAI should be extended to include the terrestrial carbon cycle (rather than just heat and moisture fluxes). Additionally, the sensitivity of crop biomes to LAI highlights a need for the better representation of crop phenology in LSMs. This, however, remains a difficult challenge as crops, in contrast to other PFTs, are strongly and directly influenced by human intervention.

5. Conclusions

The leaf area index (LAI) is a critical component of any land surface model. In this study, we performed

a sensitivity analysis of heat and carbon fluxes to perturbations in LAI using the CABLE LSM over the Australian continent on a monthly time scale. We showed that, while the influences of LAI perturbations on the heat and moisture fluxes were low, the impact on the terrestrial carbon balance was large, especially for croplands. Our results are consistent with earlier studies, which have shown that plant functional types with high interannual variability are the most sensitive to LAI perturbations, while dense vegetation is less sensitive, especially in moisture-limited regimes. A key conclusion is therefore that care should be taken in accurately prescribing LAI, particularly when simulating the carbon cycle. Clearly, assigning fixed LAI to PFTs and/or

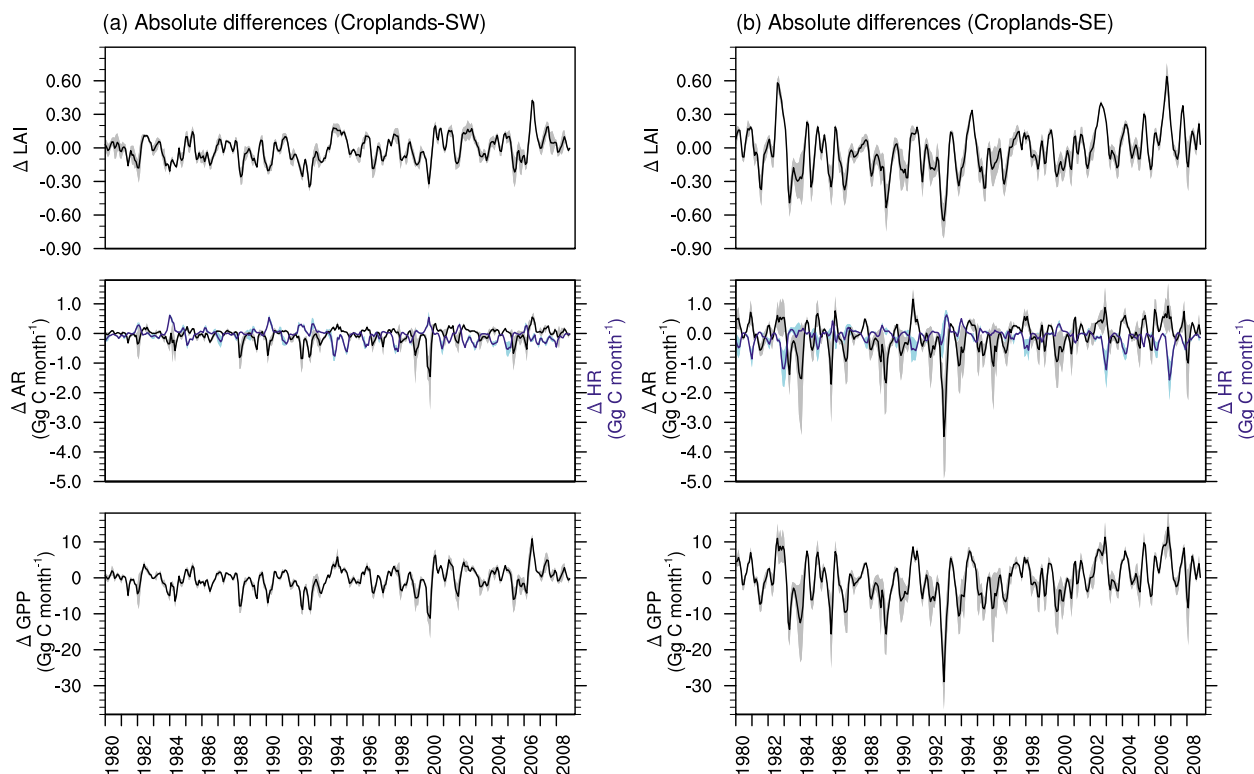


FIG. 9. Time series of monthly mean absolute differences in LAI, autotrophic respiration (AR), heterotrophic respiration (HR), and gross primary production (GPP) between the control simulation and the ensemble mean for (a) southwestern and (b) southeastern croplands.

using climatological means from remote sensing products will not accurately reflect the interannual variability of LAI, which can have a large impact on the cumulative carbon fluxes.

While our results focus on Australia, they provide several useful conclusions to the broader LSM community. First, using an ensemble of LAI products in simulations can be a very useful and straightforward method in establishing one element of uncertainty, and the method used to generate the LAI ensemble here can be adapted to other regions and/or globally. Second, there is a clear need to assess the influence of LAI on the terrestrial carbon cycle at the global scale. To our knowledge, no studies have systematically addressed this issue, and this would provide a means to better quantify the uncertainty in future changes in the global terrestrial carbon cycle. Third, the sensitivities that we find to LAI, particularly in respect of terrestrial carbon, point to the urgent need to resolve the parameterization of LAI more systematically in LSMs. Ideally, this is not through better prescriptions of LAI; rather, it is via the addition of leaf phenology modules to LSMs. This highlights an important area of development in CABLE, as well as other LSMs that have no explicit dynamical

representation of LAI. Finally, we also note that for a more complete assessment of the influence of LAI in LSMs, both the representation of vegetation through PFT maps and LAI variability should be analyzed parallel to each other.

Acknowledgments. All the authors except David Mocko are supported by the Australian Research Council Centre of Excellence for Climate System Science (CE110001028). This work was also supported by the NSW Environment Trust (RM08603). We thank CSIRO and the Bureau of Meteorology through the Centre for Australian Weather and Climate Research for their support in the use of the CABLE model. We thank the National Computational Infrastructure at the Australian National University, an initiative of the Australian Government, for access to supercomputer resources. We thank the NASA GSFC LIS team for support in coupling CABLE to LIS. The MODIS-derived background soil albedo was provided by Peter R. J. North from the Department of Geography, Swansea University, Swansea, United Kingdom. The modified MODIS LAI data were provided by Hua Yuan from the Land-Atmosphere Interaction Research Group at Beijing

Normal University. All of this assistance is gratefully acknowledged.

REFERENCES

- Abramowitz, G., and H. Gupta, 2008: Toward a model space and model independence metric. *Geophys. Res. Lett.*, **35**, L05705, doi:10.1029/2007GL032834.
- Avila, F. B., A. J. Pitman, M. G. Donat, L. V. Alexander, and G. Abramowitz, 2012: Climate model simulated changes in temperature extremes due to land cover change. *J. Geophys. Res.*, **117**, D04108, doi:10.1029/2011JD016382.
- Barr, A. G., T. Black, E. Hogg, N. Kljun, K. Morgenstern, and Z. Nestic, 2004: Inter-annual variability in the leaf area index of a boreal aspen-hazelnut forest in relation to net ecosystem production. *Agric. For. Meteorol.*, **126**, 237–255, doi:10.1016/j.agrformet.2004.06.011.
- Bonan, G. B., D. Pollard, and S. L. Thompson, 1993: Influence of subgrid-scale heterogeneity in leaf area index, stomatal resistance, and soil moisture on grid-scale land-atmosphere interactions. *J. Climate*, **6**, 1882–1897, doi:10.1175/1520-0442(1993)006<1882:IOSSHI>2.0.CO;2.
- , S. Levis, S. Sitch, M. Vertenstein, and K. W. Oleson, 2003: A dynamic global vegetation model for use with climate models: Concepts and description of simulated vegetation dynamics. *Global Change Biol.*, **9**, 1543–1566, doi:10.1046/j.1365-2486.2003.00681.x.
- Buermann, W., J. Dong, X. Zeng, R. B. Myneni, and R. E. Dickinson, 2001: Evaluation of the utility of satellite-based vegetation leaf area index data for climate simulations. *J. Climate*, **14**, 3536–3550, doi:10.1175/1520-0442(2001)014<3536:EOTUOS>2.0.CO;2.
- Chase, T. N., R. A. Pielke, T. G. F. Kittel, R. Nemani, and S. W. Running, 1996: Sensitivity of a general circulation model to global changes in leaf area index. *J. Geophys. Res.*, **101**, 7393–7408, doi:10.1029/95JD02417.
- Cruz, F. T., A. J. Pitman, and Y.-P. Wang, 2010: Can the stomatal response to higher atmospheric carbon dioxide explain the unusual temperatures during the 2002 Murray-Darling Basin drought? *J. Geophys. Res.*, **115**, D02101, doi:10.1029/2009JD012767.
- Decker, M., A. J. Pitman, and J. P. Evans, 2013: Groundwater constraints on simulated transpiration variability over south-eastern Australian forests. *J. Hydrometeorol.*, **14**, 543–559, doi:10.1175/JHM-D-12-058.1.
- Dickinson, R. E., M. Shaikh, R. Bryant, and L. Graumlich, 1998: Interactive canopies for a climate model. *J. Climate*, **11**, 2823–2836, doi:10.1175/1520-0442(1998)011<2823:ICFACM>2.0.CO;2.
- Dirmeyer, P. A., X. Gao, M. Zhao, Z. Guo, T. Oki, and N. Hanasaki, 2006: Supplement to GSWP-2: Details of the forcing data. *Bull. Amer. Meteor. Soc.*, **87** (Suppl.), doi:10.1175/BAMS-87-10-Dirmeyer.
- Dorman, J. L., and P. J. Sellers, 1989: A global climatology of albedo, roughness length and stomatal resistance for atmospheric general circulation models as represented by the simple biosphere model (SiB). *J. Appl. Meteor.*, **28**, 833–855, doi:10.1175/1520-0450(1989)028<0833:AGCOAR>2.0.CO;2.
- Duursma, R., and Coauthors, 2009: Contributions of climate, leaf area index and leaf physiology to variation in gross primary production of six coniferous forests across Europe: A model-based analysis. *Tree Physiol.*, **29**, 621–639, doi:10.1093/treephys/tpp010.
- Exbrayat, J.-F., A. J. Pitman, G. Abramowitz, and Y.-P. Wang, 2013: Sensitivity of net ecosystem exchange and heterotrophic respiration to parameterization uncertainty. *J. Geophys. Res. Atmos.*, **118**, 1640–1651, doi:10.1029/2012JD018122.
- Guillevic, P., R. D. Koster, M. J. Suarez, L. Bounoua, G. J. Collatz, S. O. Los, and S. P. P. Mahanama, 2002: Influence of the inter-annual variability of vegetation on the surface energy balance—A global sensitivity study. *J. Hydrometeorol.*, **3**, 617–629, doi:10.1175/1525-7541(2002)003<0617:IOTIVO>2.0.CO;2.
- Haverd, V., and Coauthors, 2013: Multiple observation types reduce uncertainty in Australia's terrestrial carbon and water cycles. *Biogeosciences*, **10**, 2011–2040, doi:10.5194/bg-10-2011-2013.
- Houldcroft, C. J., W. M. F. Grey, M. Barnsley, C. M. Taylor, S. O. Los, and P. R. J. North, 2009: New vegetation albedo parameters and global fields of soil background albedo derived from MODIS for use in a climate model. *J. Hydrometeorol.*, **10**, 183–198, doi:10.1175/2008JHM1021.1.
- Jones, D., W. Wang, and R. Fawcett, 2009: High-quality spatial climate data-sets for Australia. *Aust. Meteor. Mag.*, **58**, 233–248.
- Jung, M., M. Reichstein, and A. Bondeau, 2009: Towards global empirical upscaling of fluxnet eddy covariance observations: Validation of a model tree ensemble approach using a biosphere model. *Biogeosciences*, **6**, 2001–2013, doi:10.5194/bg-6-2001-2009.
- Keeling, C. D., S. C. Piper, R. B. Bacastow, M. Wahlen, T. P. Whorf, M. Heimann, and H. A. Meijer, 2005: Atmospheric CO₂ and ¹³CO₂ exchange with the terrestrial biosphere and oceans from 1978 to 2000: Observations and carbon cycle implications. *A History of Atmospheric CO₂ and Its Effects on Plants, Animals, and Ecosystems*, J. R. Ehleringer, T. E. Cerling, and M. D. Dearing, Eds., Springer Verlag, 83–113.
- Keith, H., E. van Gorsel, K. Jacobsen, and H. Cleugh, 2012: Dynamics of carbon exchange in a eucalyptus forest in response to interacting disturbance factors. *Agric. For. Meteorol.*, **153**, 67–81, doi:10.1016/j.agrformet.2011.07.019.
- Kowalczyk, E. A., Y. P. Wang, R. M. Law, H. L. Davies, J. L. McGregor, and G. Abramowitz, 2006: The CSIRO Atmosphere Biosphere Land Exchange (CABLE) model for use in climate models and as an offline model. CSIRO Marine and Atmospheric Research Paper 013, 37 pp. [Available online at www.cmar.csiro.au/e-print/open/kowalczykea_2006a.pdf.]
- Kumar, S. V., and Coauthors, 2006: Land information system: An interoperable framework for high resolution land surface modeling. *Environ. Modell. Software*, **21**, 1402–1415, doi:10.1016/j.envsoft.2005.07.004.
- , C. D. Peters-Lidard, J. L. Eastman, and W.-K. Tao, 2008: An integrated high-resolution hydrometeorological modeling testbed using LIS and WRF. *Environ. Modell. Software*, **23**, 169–181, doi:10.1016/j.envsoft.2007.05.012.
- Li, L., Y. P. Wang, Q. Yu, B. Pak, D. Eamus, J. Yan, E. van Gorsel, and I. Baker, 2012: Improving the responses of the Australian community land surface model (CABLE) to seasonal drought. *J. Geophys. Res.*, **117**, G04002, doi:10.1029/2012JG002038.
- Liu, Q., L. Gu, R. E. Dickinson, Y. Tian, L. Zhou, and W. M. Post, 2008: Assimilation of satellite reflectance data into a dynamical leaf model to infer seasonally varying leaf areas for climate and carbon models. *J. Geophys. Res.*, **113**, D19113, doi:10.1029/2007JD009645.
- Lu, X., Y.-P. Wang, T. Ziehn, and Y. Dai, 2013: An efficient method for global parameter sensitivity analysis and its applications to the Australian community land surface model (CABLE). *Agric. Forest Meteorol.*, **182–183**, 292–303, doi:10.1016/j.agrformet.2013.04.003.
- Mao, J., S. J. Phipps, A. J. Pitman, Y. P. Wang, G. Abramowitz, and B. Pak, 2011: The CSIRO Mk3L climate system model v1.0

- coupled to the CABLE land surface scheme v1.4b: Evaluation of the control climatology. *Geosci. Model Dev.*, **4**, 1115–1131, doi:10.5194/gmd-4-1115-2011.
- McColl, K. A., R. C. Pipunic, D. Ryu, and J. P. Walker, 2011: Validation of the MODIS LAI product in the Murrumbidgee catchment, Australia. *Proc. 19th Int. Congress on Modelling and Simulation*, Perth, Australia, Modelling and Simulation Society of Australia and New Zealand, 1973–1979. [Available online at <http://www.mssanz.org.au/modsim2011/E4/mccoll.pdf>.]
- Parton, W., A. Haxeltine, P. Thornton, R. Anne, and M. Hartman, 1996: Ecosystem sensitivity to land-surface models and leaf area index. *Global Planet. Change*, **13**, 89–98, doi:10.1016/0921-8181(95)00040-2.
- Piao, S., P. Friedlingstein, P. Ciais, N. Viovy, and J. Demarty, 2007: Growing season extension and its impact on terrestrial carbon cycle in the Northern Hemisphere over the past 2 decades. *Global Biogeochem. Cycles*, **21**, GB3018, doi:10.1029/2006GB002888.
- Pielke, R. A., T. J. Lee, J. H. Copeland, J. L. Eastman, C. L. Ziegler, and C. A. Finley, 1997: Use of USGS-provided data to improve weather and climate simulations. *Ecol. Appl.*, **7**, 3–21.
- Pitman, A. J., 2003: The evolution of, and revolution in, land surface schemes designed for climate models. *Int. J. Climatol.*, **23**, 479–510, doi:10.1002/joc.893.
- , M. Zhao, and C. E. Desborough, 1999: Investigating the sensitivity of a land surface scheme's simulation of soil wetness and evaporation to spatial and temporal leaf area index variability within the global soil wetness project. *J. Meteor. Soc. Japan*, **77**, 281–290.
- , F. B. Avila, G. Abramowitz, Y. P. Wang, S. J. Phipps, and N. de Noblet-Ducoudré, 2011: Importance of background climate in determining impact of land-cover change on regional climate. *Nat. Climate Change*, **1**, 472–475, doi:10.1038/nclimate1294.
- Puma, M. J., R. D. Koster, and B. I. Cook, 2013: Phenological versus meteorological controls on land-atmosphere water and carbon fluxes. *J. Geophys. Res. Biogeosci.*, **118**, 14–29, doi:10.1029/2012JG002088.
- Raupach, M. R., 1994: Simplified expressions for vegetation roughness length and zero-plane displacement as functions of canopy height and area index. *Bound.-Layer Meteor.*, **71**, 211–216, doi:10.1007/BF00709229.
- Rienecker, M. M., and Coauthors, 2011: MERRA: NASA's Modern-Era Retrospective Analysis for Research and Applications. *J. Climate*, **24**, 3624–3648, doi:10.1175/JCLI-D-11-00015.1.
- Risbey, J. S., M. J. Pook, P. C. McIntosh, M. C. Wheeler, and H. H. Hendon, 2009: On the remote drivers of rainfall variability in Australia. *Mon. Wea. Rev.*, **137**, 3233–3253, doi:10.1175/2009MWR2861.1.
- Rodell, M., and Coauthors, 2004: The Global Land Data Assimilation System. *Bull. Amer. Meteor. Soc.*, **85**, 381–394, doi:10.1175/BAMS-85-3-381.
- Saigusa, N., and Coauthors, 2008: Temporal and spatial variations in the seasonal patterns of CO₂ flux in boreal, temperate, and tropical forests in East Asia. *Agric. For. Meteorol.*, **148**, 700–713, doi:10.1016/j.agrformet.2007.12.006.
- van den Hurk, B. J. J. M., P. Viterbo, and S. O. Los, 2003: Impact of leaf area index seasonality on the annual land surface evaporation in a global circulation model. *J. Geophys. Res.*, **108**, 4191, doi:10.1029/2002JD002846.
- Verstraete, M., and R. Dickinson, 1986: Modeling surface processes in atmospheric general circulation models. *Ann. Geophys.*, **4**, 357–364.
- Wang, Y.-P., and R. Leuning, 1998: A two-leaf model for canopy conductance, photosynthesis and partitioning of available energy I: Model description and comparison with a multi-layered model. *Agric. For. Meteorol.*, **91**, 89–111, doi:10.1016/S0168-1923(98)00061-6.
- , E. Kowalczyk, R. Leuning, G. Abramowitz, M. R. Raupach, B. Pak, E. van Gorsel, and A. Luhar, 2011: Diagnosing errors in a land surface model (CABLE) in the time and frequency domains. *J. Geophys. Res.*, **116**, G01034, doi:10.1029/2010JG001385.
- , X. J. Lu, I. J. Wright, Y. J. Dai, P. J. Rayner, and P. B. Reich, 2012: Correlations among leaf traits provide a significant constraint on the estimate of global gross primary production. *Geophys. Res. Lett.*, **39**, L19405, doi:10.1029/2012GL053461.
- White, M. A., and R. R. Nemani, 2003: Canopy duration has little influence on annual carbon storage in the deciduous broad leaf forest. *Global Change Biol.*, **9**, 967–972, doi:10.1046/j.1365-2486.2003.00585.x.
- Yuan, H., Y. Dai, Z. Xiao, D. Ji, and W. Shangguan, 2011: Reprocessing the MODIS leaf area index products for land surface and climate modelling. *Remote Sens. Environ.*, **115**, 1171–1187, doi:10.1016/j.rse.2011.01.001.
- Zhang, H., L. Zhang, and B. Pak, 2011: Comparing surface energy, water and carbon cycle in dry and wet regions simulated by a land-surface model. *Theor. Appl. Climatol.*, **104**, 511–527, doi:10.1007/s00704-010-0364-x.
- , B. Pak, Y. P. Wang, X. Zhou, Y. Zhang, and L. Zhang, 2013: Evaluating surface water cycle simulated by the Australian community land surface model (CABLE) across different spatial and temporal domains. *J. Hydrometeorol.*, **14**, 1119–1138, doi:10.1175/JHM-D-12-0123.1.
- Zhang, Q., Y. P. Wang, A. J. Pitman, and Y. J. Dai, 2011: Limitations of nitrogen and phosphorous on the terrestrial carbon uptake in the 20th century. *Geophys. Res. Lett.*, **38**, L22701, doi:10.1029/2011GL049244.